REPORTS 16-02-19, 16-02-31: *STRUCTURAL STUDIES ON SKIN COLLAGEN AND ARTIFICIAL MEMBRANES, IN VITRO STRUCTURAL STUDIES: COLLAGEN AND KERATIN, AMYLOID-MEMBRANE INTERACTIONS, AND MICELLAR BEHAVIOUR OF QUILLAJA BARK SAPONIN*

The aim of these two proposals was to characterize different colloidal structures (liposomes, saponin micelles, and lipid bicelles) for biomedical applications and drug delivery, and also to quantify differences between the diffraction peaks of collagen in healthy/different pathological skin states.

Bicelles were prepared varying the lipid concentration (5, 10, 15, 20% w/w of dimiristoylphosphatidylcholine (DMPC), and dihexanoilphosphatidylcholine (DHPC)), and the lipid molar ratio (q=[DMPC]/[DHPC]=2, 2.3, 3.5) as two parameters that influence their structure. We prepared also bicelles including 10, 20% of ceramides (10c and 20c) for topical applications.
Liposomes were formed by different lipid compositions: mixtures of lipid brain extract (LB), mixtures of phosphatidylcholine (PC) with the anionic lipid phosphatidic acid (PA), and with cholesterol (Chol), sphingomyelin (SM), or both (*raft* liposomes). The mixtures of lipids mimic the cell membranes in the neuronal tissue in order to evaluate the interaction with the amyloid peptide Aβ(1-40).
Concerning to the ***skin*** samples, our first part of experimental procedures was to compare two defrosted biopsies from melanoma and from healthy skin sample. In aging or diseased skin some changes in the orientation and in the arrangement of the collagen occur. Consequently, the analysis of the collagen characteristics such as distribution and orientation can provide valuable information. On the other hand, skin layers (dermis, epidermis) were removed and analyzed separately.

The distance sample-detector was 1.4 (colloids) and 5 m (collagen), and we used capillaries for liquid samples and *kapton* windows for the skin samples.

Results and Conclusions

Bicelles

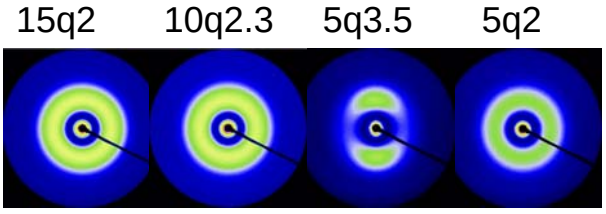

Figure 1 shows the diffraction patterns of standard bicelles DMPC/DHPC.

The results of the experiments with bicelles show that the higher the lipid concentration, the higher the intensity. We can also see some orientation for the highest q (3.5) bicelles due to the formation of a nematic phase.

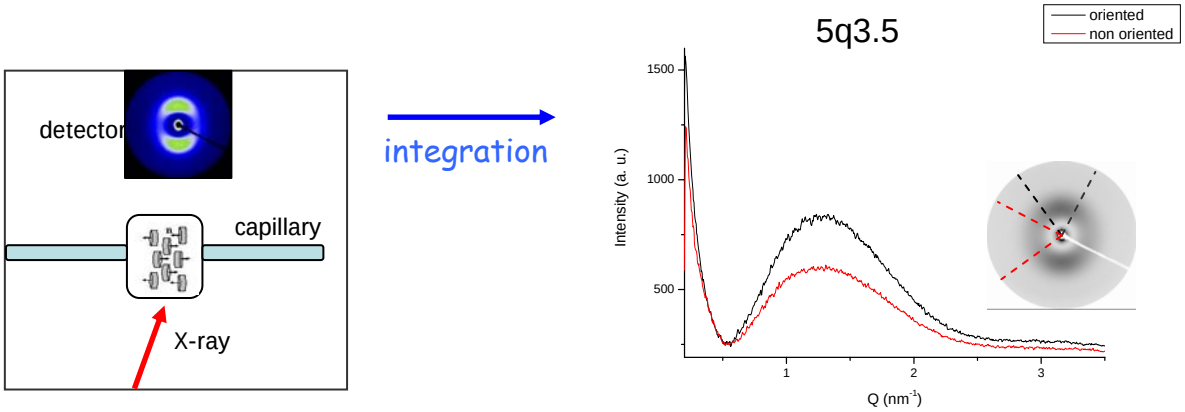

Figure 2 shows the disposition of the capillary and the X-ray beam for 5q3.5 bicelles *(left)*. Integration of the two different areas corresponds to the meridional and the equatorial plane of the scattering pattern *(right).*

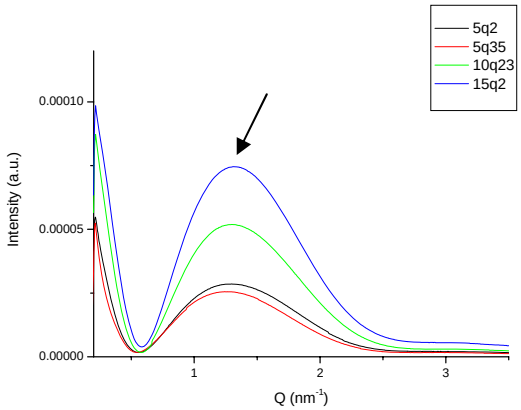

Figure 3. Curves obtained from the integration of the spectra of the figure 1. The samples were corrected by the background solution.

The standard bicelles showed a broad band centred at Q~1.3 nm^{-1} (Figure 3) resulting from non-ordered structures. These bands could be explained as the contribution of the form factor of single bicelles, with low interparticle interaction. The maximum intensity of the broad band for bicelles q=3.5 is centred at around the same Q than for the isotropic bicelles (q=2, 2.3). The Q~1.3 nm^{-1} could be related to the thickness of DMPC bilayer (~4 nm^{-1}), which is the same in all the cases.

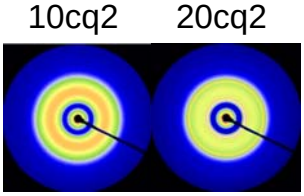

Figure 4. Diffraction patterns of bicelles 20q2 in which, the long-chain phospholipid (DMPC) is substituted by 10 or 20% of Cer (10cq2, 20cq2).

These bicelles also form isotropic phases but show more complex spectra. 10cq2 bicelles present the band centred at Q~1.3 nm^{-1} (figure 5) and a little shoulder at Q~0.9 nm^{-1}. The scattering curve of 20cq2 bicelles shows three peaks (Q=0.9, 1.8,

2.7 nm^{-1}), and the band at Q~1.3 nm^{-1}, indicating a mixture of ordered and non-ordered aggregates in the sample. A d-spacing of 6.9 nm could correspond with a d-spacing of lipid bilayers containing ceramides (longer molecule than DMPC).

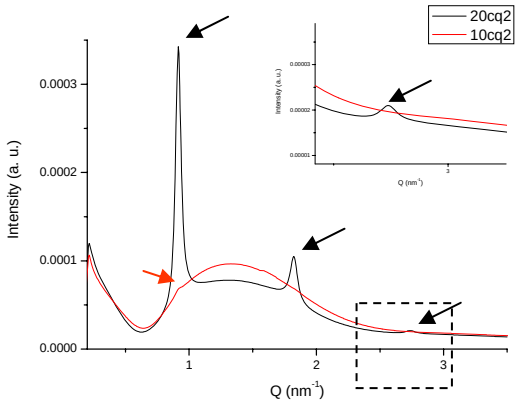

Figure 5. Curves obtained from the integration of the spectra of the figure 4. The samples were corrected by the background solution.

Up to 10% of ceramides seems that not modify bicelles, keeping the characteristic broad band, but when a 20% of ceramides is added, a mixture of structures appears: stacking bilayers with a d-spacing of 6.9 nm formed mainly by ceramides, besides the non-ordered phase (bicelles) formed by DMPC, DHPC and less of 10% of ceramides.

Liposomes with the amyloid peptide Aβ(1-40)

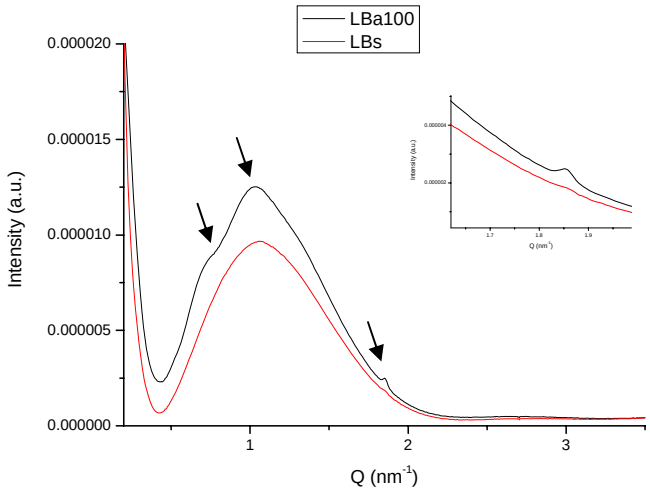

Figure 6. Curves obtained from the integration of the spectra of LB liposomes, and LB with amyloid peptide Aβ(1-40)

LB liposomes present a band centred at Q~1.06 nm^{-1}. The Aβ(1-40) addition promotes a slight change in the band position (centred at Q ~1.03 nm^{-1}), appears a shoulder centred at Q~0.7 nm^{-1}, and a small peak at Q~1.85 nm^{-1} (see the insert). In this case, Aβ(1-40) induces some order in the membranes: it could be due to an effect of binding caused by the peptide on the membranes.

Figure 7. Curves obtained from the integration of the spectra of liposomes form by a mixture of PC:Chol:SM (*raft*) with Aβ(1-40), and PC, PC:PA.

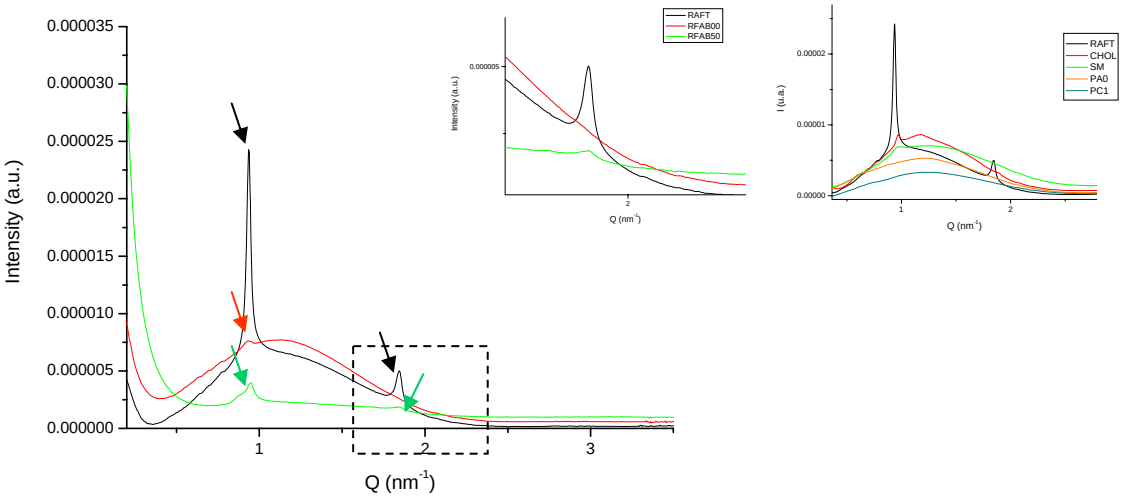

Experiments with Aβ(1-40) resulted in a wide number of SAXS patterns. Liposomes formed by PC, PC:PA show broad bands characteristic of non-ordered structures, in the same way of LB. The amyloid peptide addition modifies the SAXS pattern inducing the apparition of peaks at different positions overlapping on the band. Conversely, liposomes with Chol, and/or SM present some ordered structures (peaks) and the addition of Aβ(1-40) seems that promote a decrease in the order. In summary, amyloid peptide interacts with membranes producing different effects depending on the composition.

Skin

Figure 8. Comparison of two defrosted biopsies from melanoma and from healthy skin.

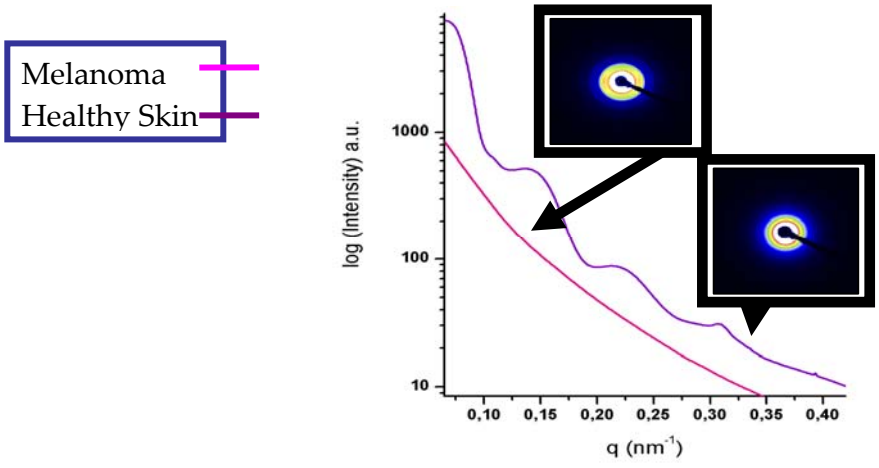

As it is shown in the figure 8, there are clear differences between both samples. Melanoma biopsy lost all the peaks corresponding to the different collagen diffractions; however these peaks are clearly presents on the healthy skin diffractogram. We observed that both the melanoma and the healthy skin samples presented different scattering patterns, consequently we proceed to see if it was possible to use the same methodology usually used in histopathological laboratories.

Samples embedded in paraffin: after eliminated the paraffin by soaking the samples in different organic solvents, we doubt how the organic solvents could affect the composition and structure of the skin, so we preferred to change this methodology and to test the skin samples embedded in paraffin without any posterior treatment.

Melanoma and healthy skin biopsies showed the same patterns that the ones obtained with defrosted samples.
Figure 9. SAXS scans on the surroundings of melanoma.

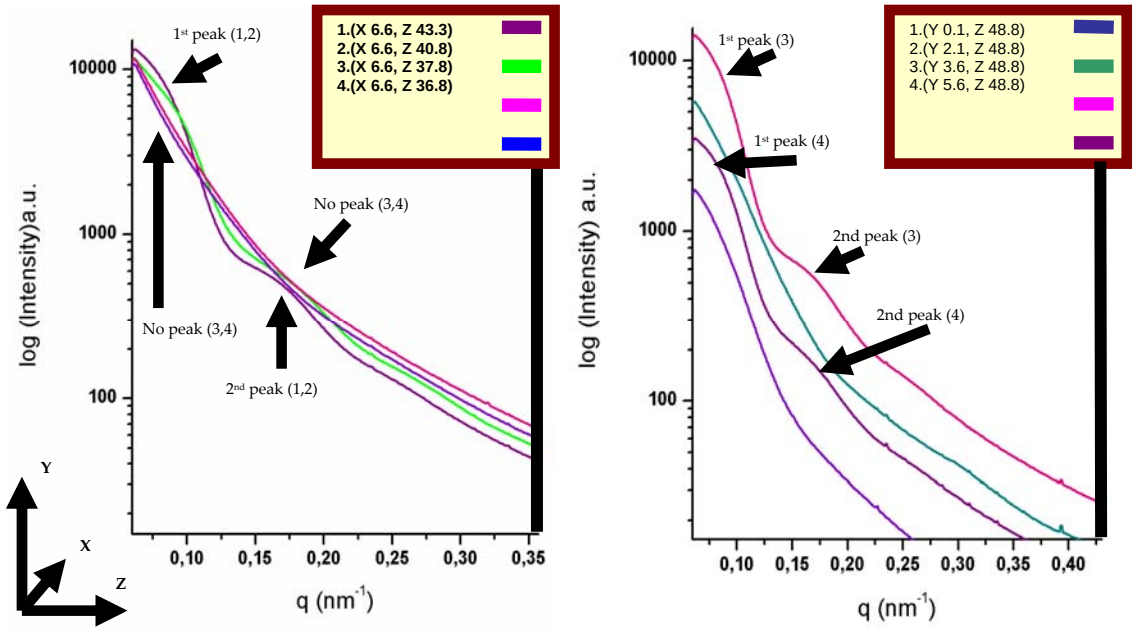

Thanks to this evidence we decided to carry out different scans of each sample in order to compare the melanoma invaded areas to non-invaded ones.
Both figures show very clear differences between the diffractograms obtained from the skin affected by melanoma and the surrounding (apparently healthy skin).

Figure 10. Curves obtained from the integration of the skin spectra: whole skin, epidermis, and dermis. Distance sample-detector was 1.4 m. The samples were corrected by the capillary.

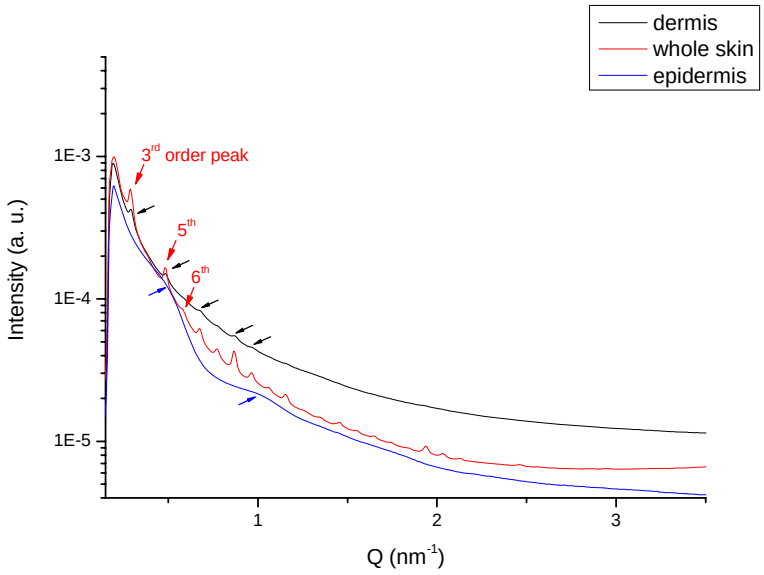

At 1.4 m configuration, the whole skin curve presents the 3rd, 5th ,and 6th order peaks of SAXS pattern collagen, among others at high Q. The dermis curve doesn't show the 6th order peak and differ from the skin curve at the intensity of peaks. The epidermis curve only shows some bands. The thickness of the skin layers couldn't be controlled.

Figure 11. Curves obtained from the integration of the skin spectra: whole skin, epidermis, and dermis. Distance sample-detector was 5 m. The samples were corrected by the capillary.

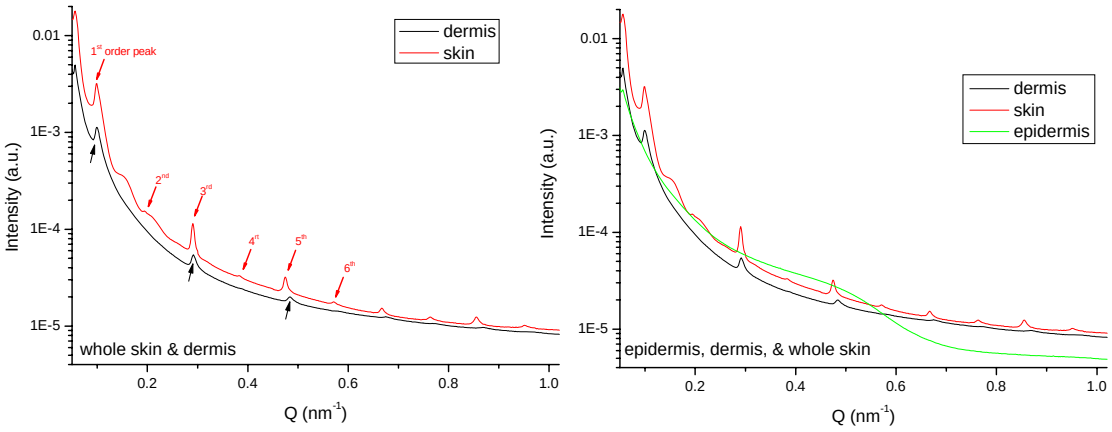

In this case, we can see more than 6th order peak of SAXS diffraction pattern in the skin sample, and less in the others layers of skin. We can conclude that SAXS is a very powerful tool for characterizing the skin.